The Two Competitive Photodissociation Channels in Cyano Carbonyls (NCC(O)X, X = CH_3, $CH(CH_3)_2$, $C(CH_3)_3$, OCH_3) at 193 nm. A Study by Photofragment Translational Energy Spectroscopy

Alan Furlan, Heiner A. Scheld, and J. Robert Huber*

Physikalisch-Chemisches Institut der Universität Zürich, Winterthurerstrasse 190, CH-8057 Zürich, Switzerland

Received: September 29, 1999; In Final Form: December 20, 1999

The photodissociation of a series of four cyano carbonyl compounds NCC(O)X with X = methyl, isopropyl, *tert*-butyl, and methoxy was studied after excitation at 193 nm using photofragment translational energy spectroscopy. For all the fragments generated (OCCN, XCO, CO, CN, X) the kinetic energy distributions were measured and the two radical decay channels, NCC(O)X → CN + OCX and NCC(O)X → OCCN + X, were identified. Dissociation leading to CN + OCX is the main decay path (∼85%) for acetyl cyanide (X = methyl), but is the minor pathway for X = isopropyl (30%), X = *tert*-butyl (17%), and X = methoxy (<5%). The primary fragments CN + OCX were found to be stable with respect to secondary dissociation in all cases, except for acetyl cyanide which exhibits spontaneous fragmentation of the acetyl fragments to CH_3 + CO with a yield of ∼9%. The stability of the remaining acetyl + CN fragment pairs is probably due to electronic excitation of one of the fragments. Elimination of X is the major decay path for X = methoxy, and the anisotropic recoil distribution of the fragments suggests the decay to be fast on the time scale of a parent rotation. Within the homologous series X = methyl, isopropyl, and *tert*-butyl the propensity for X elimination, and thus OCCN production, increases with the size of the alkyl moiety. The observed trend toward increasing fragment internal energy with increasing size of the alkyl fragment indicates a considerable amount of randomization of the excess energy prior to bond scission. The investigation of the four compounds proved methyl cyanoformate to be the most favorable species for an efficient photolytical production of *stable* OCCN radicals, whereas acetyl cyanide is the most efficient source of CN radicals within this series.

1. Introduction

The ultraviolet photodissociation of many carbonyl compounds following the decay path denoted as Norrish type I dissociation, has attracted much attention leading to numerous experimental and theoretical investigations.[1−3] For photodissociation taking place on asymmetrically substituted carbonyl compounds the interesting question of bond selectivity and energy partitioning arises. In general, for asymmetrically substituted ketones the weaker of the two α-C−C bonds is broken. This cleavage occurs on the nπ* triplet potential energy surface which has a barrier along the reaction coordinate due to an avoided crossing with a higher lying potential surface. The α-C−C bond with the smaller reaction barrier on the triplet surface is then preferentially broken.[3,4] Different behavior is observed for nonalkyl substituted carbonyls. Thus UV photodissociation of acetyl chloride shows cleavage exclusively of the C−Cl bond despite of both α-bonds having a similar bond energy.[5−8] This α-bond selectivity was explained by the C−Cl dissociation proceeding on the initially excited potential surface while that of the C−C bond occurrs only after a relatively slow intersystem crossing to the ^{3}(nπ*) surface. In the photodissociation of acetyl bromide[9,10] and iodide[11] a similar situation is encountered. Also the decay pathway of acetic acid appears unusual in that the OH elimination is strongly favored over CH_3 elimination even though the C−CH_3 bond is weaker than the C−OH bond.[12−14] Similarly and of direct relevance to the present work, acetyl cyanide ($CH_3C(O)CN$) has been found to dissociate at 193 nm selectively to CH_3CO + CN[15,16] despite ab initio calculations predicting the bond dissociation energies to be D_0(C−CN) = 427 kJ/mol and D_0(C−CH_3) = 360 kJ/mol.[16]

Beside the elucidation of mechanistic features of cyano carbonyls this work was stimulated by recent investigations of photochemical sources of stable OCCN radicals, a species of potential interest in atmospheric chemistry.[17,18] As has recently been shown by photofragment translational energy spectroscopy, the OCCN radical is the major product formed in gas-phase photodissociation of carbonyl cyanide, $CO(CN)_2$.[19,20] The unimolecular decay of this compound to OCCN + CN is the dominant dissociation channel (94 ± 2%) after excitation at 193 nm. About 18 ± 6% of the nascent OCCN fragments possess sufficient internal energy to overcome the barrier to secondary dissociation producing CO + CN during the flight time from the reaction zone to the detector. In competition with the primary radical decay is the molecular decay or elimination reaction where the excited carbonyl cyanide dissociates into CO + $(CN)_2$. This channel was found to have a yield of about 6 ± 2%. Thus under our photodissociation conditions stable OCCN radicals can be produced with a yield of about 77 ± 6%.[20]

With the present study we investigated the photodissociation mechanism of several closely related cyano carbonyl compounds NCC(O)X (Figure 1). The recent investigations on acetyl cyanide (X = CH_3)[15,16,21,22] were refined and previously unobserved photodissociation products identified. A homologous series of compounds with X = alkyl were studied where acetyl

* Corresponding author. Telephone: 0041-1-6354460. Fax: 0041-1-6356838. E-mail: jrhuber@pci.unizh.ch.

10.1021/jp9934836 CCC: $19.00
Published on Web 02/10/2000

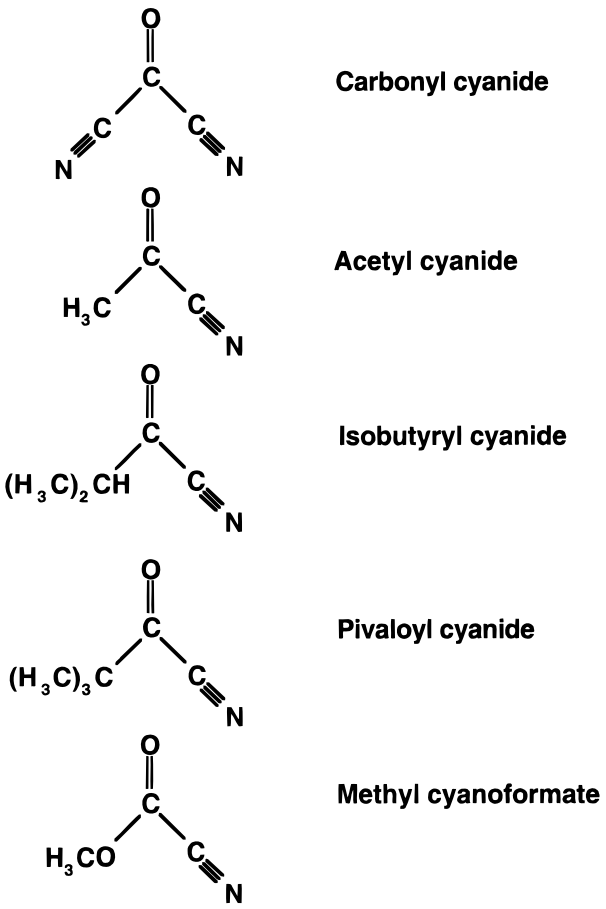

Figure 1. Investigated NCC(O)X compounds.

cyanide constitutes the simplest member. Of particular interest is the identification of changes in the selectivity or propensity of the α-C−C bond rupture as X = methyl is replaced by isopropyl and *tert*-butyl, and thus to find the compound with the highest yield of stable OCCN radicals. In this context we have included in our study the methoxy compound (X = OCH_3). This promises to be another species which favors scission of the stronger C−OCH_3 bond as expected from findings with acetic acid.[12−14]

After excitation the NCC(O)X molecules given in Figure 1 (X = methyl, isopropyl, *tert*-butyl, or methoxy) are subject to the following primary dissociation steps:

$$NCC(O)X + h\nu \rightarrow OCX + CN \quad (1)$$

$$NCC(O)X + h\nu \rightarrow NCCO + X \quad (2)$$

If the dissociation process channels sufficient internal energy into the fragments, reactions 1 and 2 may be followed by secondary decays. Alternative pathways to the radical decays (1) and (2) are the molecular channel (3):

$$NCC(O)X + h\nu \rightarrow CO + NCX \text{ (or CNX)} \quad (3)$$

and the concerted three-body decay (4):

$$NCC(O)X + h\nu \rightarrow CO + CN + X \quad (4)$$

In this dissociation process the excited molecule decays to three final fragments with the cleavage of two bonds occurring in a single kinetic step.[23,24]

Using photofragment translational energy spectroscopy (PTS) we have investigated the photochemical decay of the three acyl cyanides introduced above and methyl cyanoformate (Figure 1) at 193 nm (619 kJ/mol). We were able to detect all fragments (OCCN, X, XCO, and CN) generated via the radical decay channels (1) and (2) and to measure their kinetic energy distributions using different scattering angles. For methyl cyanoformate the recoil anisotropies of the OCCN and CN fragments were also determined.

TABLE 1: Stream Velocities and Widths Determined for the NCC(O)X Compounds Studied in the Carrier Gas He

compound	[vol %]	stagnation pressure [mbar]	stream velocity v_s [m/s]	width α [m/s]
$NCC(O)CH_3$	5	350	1610 ± 70	138 ± 4
$NCC(O)CH(CH_3)_2$	2	350	1700 ± 50	127 ± 3
	5	200	1140 ± 90	170 ± 6
$NCC(O)C(CH_3)_3$	2	350	1315 ± 65	125 ± 7
	5	350	1300 ± 60	96 ± 4
$NCC(O)OCH_3$	2	350	1575 ± 80	103 ± 6
	6	350	1280 ± 100	99 ± 11

2. Experimental Section

The experiments were carried out with a photofragment translational energy spectrometer which has been described in detail elsewhere.[25] It consists of a rotatable, pulsed molecular beam source, a 34.5-cm long drift tube, and a quadrupole mass spectrometer for mass filtering and detection. The experiments were performed at 193 nm with an ArF excimer laser (Lambda Physik Compex 102) operated at 20 Hz providing a laser fluence between 60 and 600 mJ/cm^2. The photolysis laser beam crossed the molecular beam at a distance of 65 mm from the piezoelectric pulsed nozzle. The laser beam was slightly focused to a spot size of 6 × 2 mm^2 at the intersection with the molecular beam.

The time-of-flight (TOF) distributions were recorded at scattering angles Θ = 9°, 30°, and 18° or 45°, where Θ represents the angle between the molecular beam and the detection axis. For Θ = 9° the background signal from parent molecules was substantial and had to be subtracted on a shot-to-shot basis by leaving every second molecular beam pulse unphotolyzed. The TOF distributions shown below were corrected for the ion flight time through the mass filter. The anisotropy measurements were carried out at six different polarization angles between the electric field vector and the detection axis. The laser light was linearly polarized (polarization degree of 92 ± 1%) by directing the laser beam through a stacked-plates polarizer followed by a zeroth-order half-wave retarder. A measurement was repeated several times to minimize the influence of long-term drifts and the runs were corrected for the laser power fluctuations.

Acetyl cyanide, pivaloyl cyanide, and methyl cyanoformate (see Figure 1) were purchased from Fluka with purities of 98.5, 97, and 95%, respectively. Isobutyryl cyanide was obtained by the reaction of isobutyryl chloride with sodium iodide in acetonitrile at 25 °C, followed by the reaction of the product isobutyryl iodide with copper cyanide in CH_2Cl_2 at 90 °C.[26,27] Expansions of the premixed gas samples of 2−6% NCC(O)X seeded in helium carrier gas at a total stagnation pressure of 200−350 mbar were used throughout this study. The molecular beam velocity distribution $f(v) \sim v^2 \exp[-(v - v_S)^2/\alpha^2]$ was determined before and after each measurement, using a chopper wheel synchronized with the pulsed valve. The stream velocity v_S and the width α for all mixtures are given in Table 1. To check and avoid cluster formation of NCC(O)X in the molecular beam and multiphoton processes, we recorded TOF spectra with

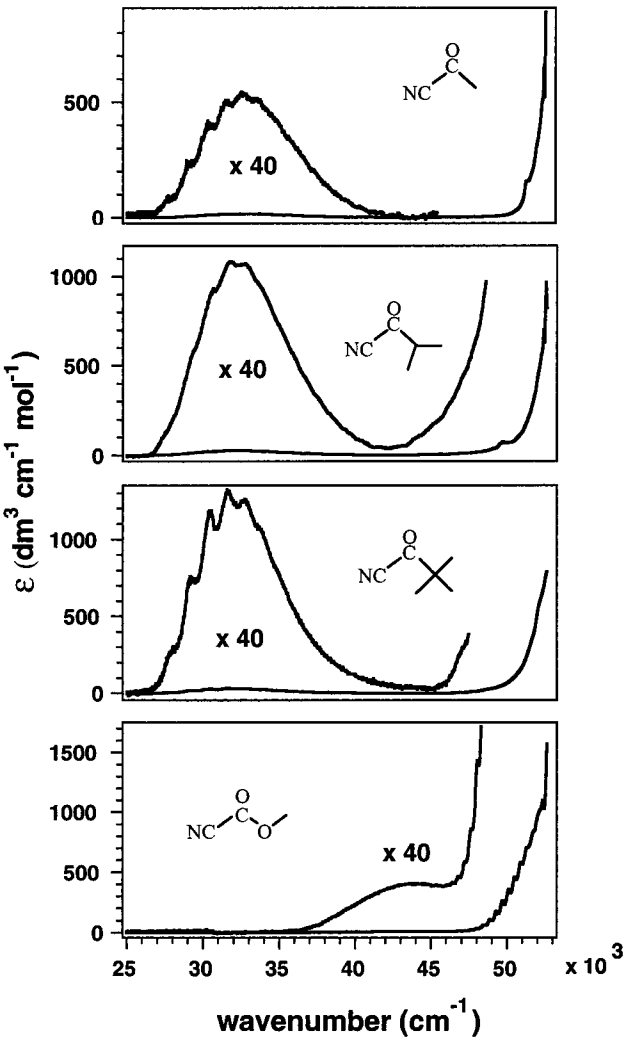

Figure 2. Gas-phase absorption spectra of NCC(O)X, X = CH_3, $CH(CH_3)_2$, $C(CH_3)_3$, and OCH_3 in the wavelength region 190−410 nm. The spectra were recorded at room temperature, using a vapor pressure of 2 mbar and a resolution of about 0.2 nm (fwhm).

varying NCC(O)X concentrations between 0.5 and 10% and with the laser power changing from 60 to 600 mJ/pulse.

3. Results

A. UV Spectra. The alkylated cyano carbonyl compounds with X = CH_3, $CH(CH_3)_2$, and $C(CH_3)_3$ exhibit very similar UV absorption spectra in the range 190−410 nm as shown in Figure 2. The weak bands centered at 310 nm are attributed to the $S_0 \rightarrow S_1$ ($n\pi^*$) transition localized on the CO group.[28,29] The coarse structure of a vibronic progression, which in the spectra of the compounds with X = $CH(CH_3)_2$ and $C(CH_3)_3$ peaks at the fourth member of the progression ($\nu \approx 1260$ cm^{-1}), in the spectrum of X = CH_3 at the fifth member ($\nu \approx 1360$ cm^{-1}), is assigned to the C═O stretching vibration in the S_1 state as guided by the fully assigned progressions in related carbonyl compounds such as acetone.[30] Beside the weak $n\pi^*$ transition the spectra exhibit a steep onset of the absorption below 220 nm with an absorption cross section at 193 nm of 200−400 dm^3 mol^{-1} cm^{-1}. In acetyl cyanide, North et al.[15] tentatively assigned this strong absorption to the ^{1}(n,3s) transition in analogy with the absorption of acetone in this wavelength region, which involves the promotion of a lone-pair electron of oxygen to the 3s Rydberg state. Very recently Owrutsky and Baronavski proposed a $\pi\pi^*$ transition to be responsible for the

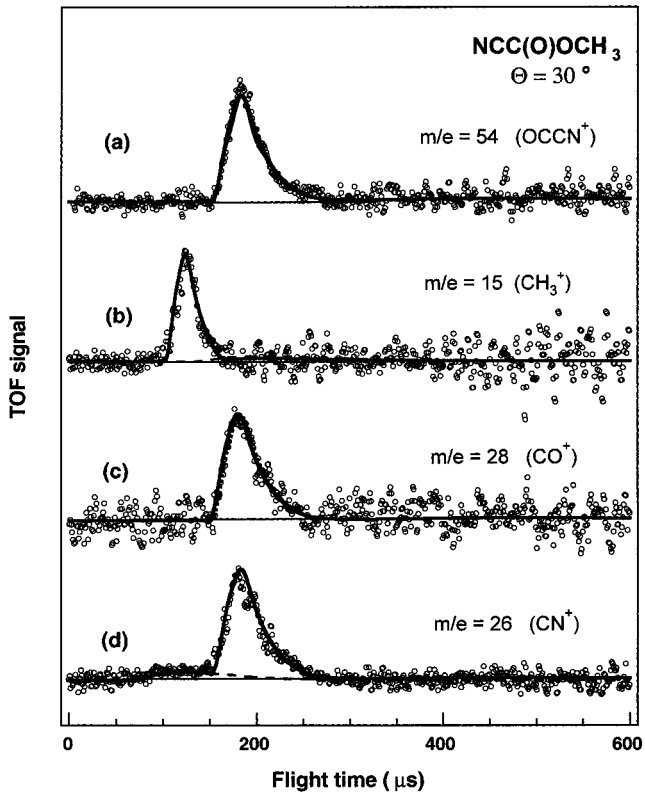

Figure 3. Unpolarized TOF distributions of the photofragments of methyl cyanoformate after excitation at 193 nm for $OCCN^+$ (a), CH_3^+ (b), CO^+ (c), and CN^+ (d). The dotted lines were calculated from the translational energy distribution $P(E_T)$ shown in Figure 4a for decay channel (2). The dashed lines were obtained from $P(E_T)$ for channel (1) displayed in Figure 6a. The solid lines represent the best fit by weighting both decay channels.

193 nm absorption of acetyl cyanide involving the promotion of an electron from the π orbital on CN to the π^* orbital localized on CO.[31] Since the different alkyl substituents have only a weak effect on the electronic transition localized on the partially conjugated OCCN moiety, we expect the assignment of the 193 nm absorption (either (n,3s) or ($\pi\pi^*$)) to be the same for all three alkyl compounds with X = methyl, isopropyl, or *tert*-butyl.

The absorption spectrum of methyl cyanoformate (Figure 2, bottom) exhibits a strongly blue-shifted $n\pi^*$ band centered at 230 nm. This blue shift, also expected for the $\pi\pi^*$ and Rydberg states at higher energies, is typical for esters and even larger for carboxy acids, as discussed by Robin.[28] However, in a photodissociation study of acetic acid, Hunnicutt et al.[13] argued that the absorption at 200 nm is still part of the ^{1}($n\pi^*$) transition. Based on these available data it is presently not possible to give a conclusive assignment to the 193 nm absorption of methyl cyanoformate.

B. TOF Spectra of $NCC(O)OCH_3$. We start with the photodissociation results of methyl cyanoformate since it turned out to be the suitable reference species to determine the contributions of the CN^+ and CO^+ products to the overall TOF spectra. After excitation at 193 nm, the photofragment time-of-flight data were found at $m/e = 54$ ($OCCN^+$), 28 (CO^+), 26 (CN^+), 15 (CH_3^+), and 59 (H_3COCO^+). It is noted that no signal was detected at $m/e = 31$ (H_3CO^+). The TOF spectra of the four fragment species generated, $OCCN^+$, CO^+, CN^+, and CH_3^+, are displayed in Figure 3.

As OCCN can only originate from the primary dissociation step (2), the unambiguous TOF data for the OCCN fragments

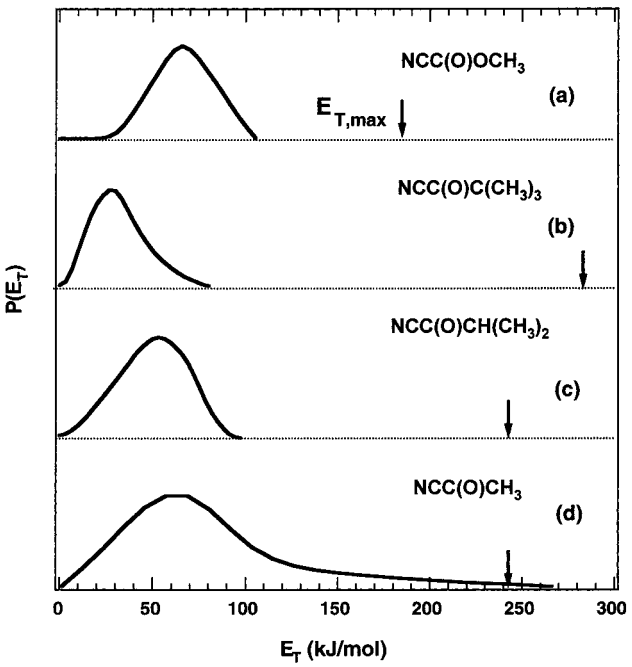

Figure 4. Center-of-mass translational energy distributions $P(E_T)$ for the decay NCC(O)X → OCCN + X (2) of methyl cyanoformate (a), pivaloyl cyanide (b), isobutyryl cyanide (c), and acetyl cyanide (d). The arrows mark E_{avl} of the fragment pairs as calculated with the ab initio dissociation energies given in Table 2.

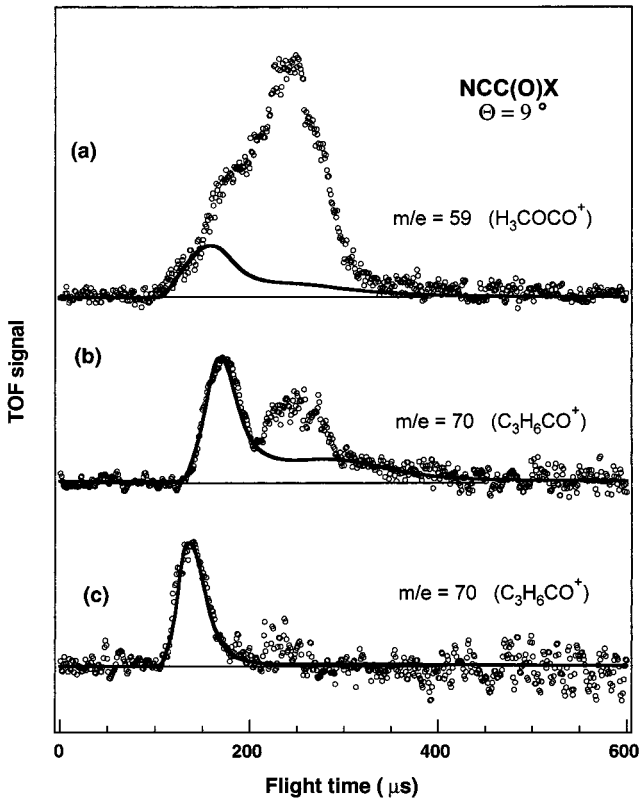

Figure 5. Unpolarized TOF spectra of the OCX fragments from methyl cyanoformate (a), pivaloyl cyanide (b), and isobutyryl cyanide (c) after excitation at 193 nm for H_3COCO^+ (a), $H_6C_3CO^+$ (b), and $H_6C_3CO^+$ (c). The solid lines were calculated from $P(E_T)$ shown in Figure 6.

were analyzed first using the forward convolution[32] of the center-of-mass kinetic energy distribution $P(E_T)$ shown in Figure 4a. This best fit of the spectra is represented by the solid line in Figure 3a. In the following this $P(E_T)$ was checked by comparison with the TOF spectra of the counterfragment H_3CO which, although not observed, manifests itself by the cracking fragments CH_3 and O formed in the ionizer. In previous studies the H_3CO radical was also found to be completely cracked in the ionizer.[33−35] Based on the strict momentum-correlation of the fragment pairs OCCN and H_3CO, the latter distribution represented by CH_3 at mass 15, provided an excellent fit to the TOF data Figure 3b. This result also implies that the primary product H_3CO is completely fragmented in the ionizer to CH_3 + O. The spectrum Figure 3c recorded at m/e = 28 (CO^+) could be fitted by a single CO^+ component which stems from cracking of $OCCN^+$ to CO^+ + CN in the detector. Furthermore the experiments carried out at scattering angle Θ = 9° allowing sensitive detection of very slow fragments showed no discernible deviation between the momentum matched OCCN and CH_3 signals which indicates that all emerging OCCN photoproducts are stable with respect to spontaneous dissociation to CN + CO.

If methyl cyanoformate dissociates exclusively to H_3CO and OCCN according to reaction 2, the TOF spectra shown in Figure 3 should be fitted by a single $P(E_T)$ distribution. While this is the case for the spectra a, b, and c, the spectrum d recorded at m/e = 26(CN^+) revealed a small additional contribution between 75 and 150 μs prior to the fast rising edge. Since this contribution persisted after decreasing the laser power by a factor of 10, it could not stem from a two-photon absorption process but rather from reaction channel (1). Thus to fit the CN^+ spectrum two components were required: first, the CN from cracking of $OCCN^+$ in the detector (main contribution above 150 μs in Figure 3d), and second, CN from the dissociation of the parent molecule to H_3COCO and CN (1). This latter CN signal could only be clearly observed in the TOF spectra at Θ ≥ 30°. At smaller scattering angles the CN channel (1) contribution overlaps strongly with the CN signal from OCCN cracking.

The counterfragment of these fast CN radicals from channel (1) should appear at m/e = 59 (H_3COCO^+). An appreciable signal was however detected only under relatively high parent molecule concentrations (i.e., 10% methyl cyanoformate at 350 mbar stagnation pressure) and is shown in Figure 5 as curve a. With the $P(E_T)$ for the fast CN radicals (dashed line in Figure 3d) we obtained after momentum-matching and Θ adaption the distribution of its counterfragment H_3COCO (solid line in Figure 5a) which fits the rising edge of the TOF spectrum m/e = 59 very well. This distribution provided the $P(E_T)$ shown in Figure 6a. The overall fit including both CN contributions is represented by the solid line in Figure 3d. To estimate the relative efficiencies of the reaction channels (1) and (2) from the respective CN yields it is necessary to know the cracking pattern of the OCCN fragments in the ionizer. This is obtained from the present methyl cyanoformate data where the signals of the fragment masses m/e = 26 (CN^+) and m/e = 28 (CO^+), after correction for the clearly separated channel (1) contribution, originate exclusively from OCCN cracking in the ionizer. Comparison of the relative intensities of the CO, CN, and OCCN fragment signals shows that 55 ± 10% of the ionized OCCN are detected at m/e = 54 and the rest is cracked, 30 ± 10% to CN^+ + CO and 15 ± 10% to CN + CO^+. (The velocity and mass dependence of the ionization efficiency were taken into account.) From the TOF spectrum Figure 3d the relative weights of the two CN^+ contributions are found to be 6:1. Since in the case of channel (2) only 30% of OCCN appear as CN^+, we finally obtain a branching ratio of channel (2)/channel (1) ≈ 20. Thus, about 95% of the excited parent molecules decay along channel (2) and about 5% along channel (1). We should note

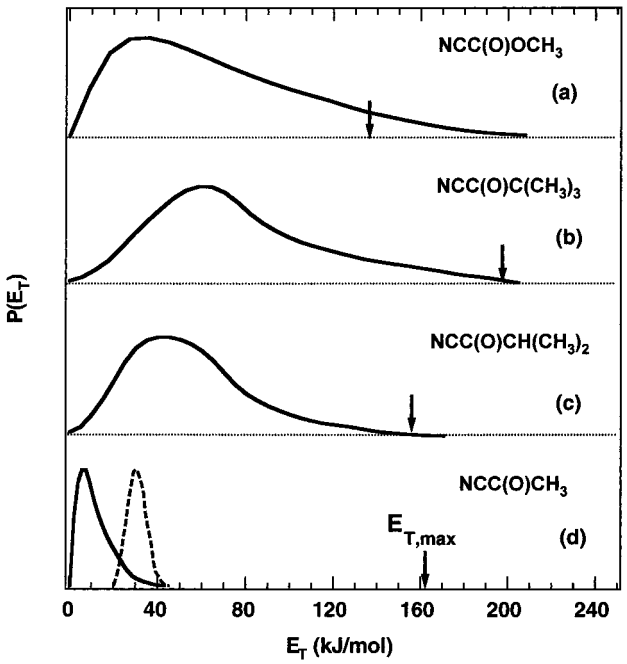

Figure 6. Center-of-mass translational energy distributions $P(E_T)$ for the decay NCC(O)X → CN + OCX (1) of methyl cyanoformate (a), pivaloyl cyanide (b), isobutyryl cyanide (c), and acetyl cyanide (d). The dashed line in Figure 6d represents the primary $P(E_T)$ of the unstable acetyl radicals. The arrows mark E_{avl} of the fragment pairs.

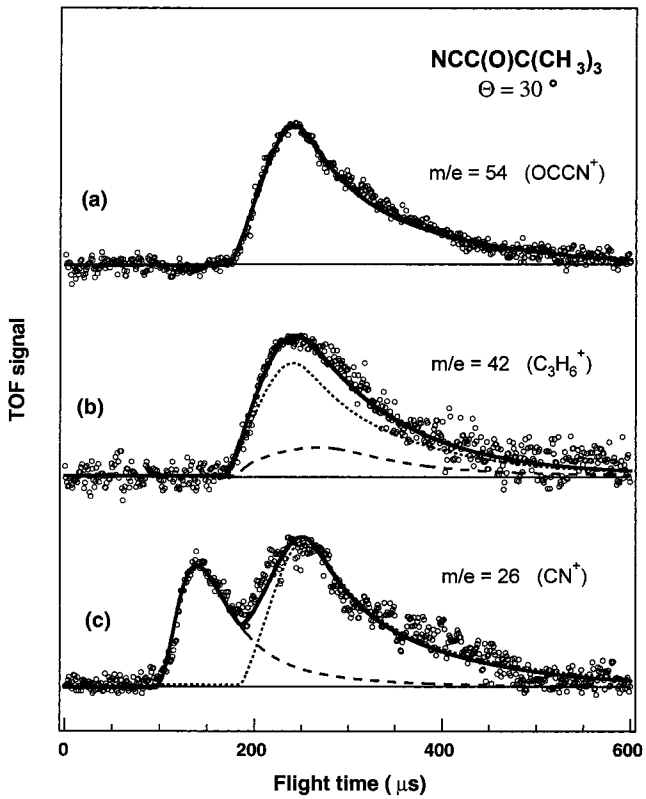

Figure 7. Unpolarized TOF spectra of the photofragments of pivaloyl cyanide after excitation at 193 nm for $OCCN^+$ (a), $C_3H_6^+$ (b), and CN^+ (c). The solid line in (a) and the dotted lines in (b) and (c) were obtained with the $P(E_T)$ from Figure 4b and the dashed lines in (b) and (c) with those from Figure 6b. The solid lines in (b) and (c) represent the sum of contributions from both decay channels.

that in Figure 3b,c the fit indicated by the strong line was obtained without consideration of the small channel (1) contribution. This is expected to appear at long flight times where, however, the signal/noise ratio is no longer sufficient to discern the effect.

The fragment recoil anisotropy β was determined from the polarization dependence of the TOF signal measured at $\Theta = 30°$, $m/e = 54$ ($OCCN^+$), and $m/e = 26$ (CN^+). The signals at the other masses were not strong enough for polarized measurements. For both masses the analysis yielded $\beta = 0.8 \pm 0.1$, which implies the dissociation to occur on a time scale shorter than one rotational period of the parent molecule.[36]

C. TOF Spectra of $NCC(O)C(CH_3)_3$ and $NCC(O)CH(CH_3)_2$. The results of these two compounds are similar. We first consider those of pivaloyl cyanide ($X = C(CH_3)_3$). After excitation at 193 nm, time-of-flight signals of photofragments were found at $m/e = 54$ ($OCCN^+$), 26 (CN^+), 42 ($C_3H_6^+$), and 70 ($H_6C_3CO^+$); the TOF spectra of the OCCN, CN, and C_3H_6 fragments are displayed in Figure 7. The analysis procedure was identical to that described for the methyl cyanoformate above. First we analyzed the spectrum consisting of only one component, namely $OCCN^+$ (Figure 7a), and obtained the center-of-mass $P(E_T)$ distribution (Figure 5b) using forward convolution.[32] This $P(E_T)$ was then inspected by comparison with the TOF spectrum of the momentum-correlated *tert*-butyl counterfragment. Because of extensive cracking of this alkyl fragment in the ionizer, the mass filter setting at $m/e = 42$ ($C_3H_6^+$) instead at 57 ($C_4H_9^+$) yielded a better signal-to-noise ratio for its detection (The different flight times of the ions through the detector were taken into account.). Although the distributions of OCCN and of the alkyl rest provide a good fit to the spectra Figure 7a,b, the latter is actually composed of two components as revealed by the CN^+ TOF spectrum described below. The correct best fit of the spectrum Figure 7b including the contribution of channel (2) is represented by the solid line.

The CN^+ spectrum of Figure 7c exhibits two clearly distinguishable contributions with maxima at about 135 and 250 μs flight time. The slower contribution stems from $OCCN^+$ cracking and is represented by the dotted line, while the fast one indicated by the dashed line originates directly from channel (1) dissociation. To examine this decay channel we also collected data at $m/e = 70$ ($H_6C_3CO^+$) which corresponds to the $H_9C_4CO^+$ fragments cracked in the ionizer. This heavy fragment could, however, only be detected at small scattering angles ($\Theta = 9°$) as shown in Figure 5b. The spectrum consists of two peaks at 170 μs and around 240 μs where the latter turned out to be from clusters which disappeared after reduction of the parent molecule concentration. The first peak was found to correlate to the fast peak in the CN^+ spectrum of Figure 7c as demonstrated by the strong line in Figure 5b. Thus the $P(E_T)$ shown in Figure 6b is—after momentum-matching—the same for CN^+ from channel (1) and ($H_9C_4CO^+$).

To calculate the fit for the overall spectrum indicated by the solid lines in Figure 7, the branching ratio between the decay channels (1) and (2) has to be known. This was estimated from the two CN^+ contributions in the TOF spectrum Figure 7c taking into account the OCCN cracking pattern determined above. We calculated the ratio channel (2)/channel (1) ≈ 5. Thus about 83% of the excited parent molecules decay along channel (2) and about 17% along channel (1). This estimation rests on the assumption that $NCC(O)OCH_3$ and $NCC(O)C(CH_3)_3$ have the same cracking patterns with respect to OCCN. The second uncertainty is due to a possible spontaneous decay of the OCCN and the H_9C_4CO fragments during the flight from the reaction zone to the detector. As we could not find any deviations between the spectra of the OCCN and alkyl fragments,

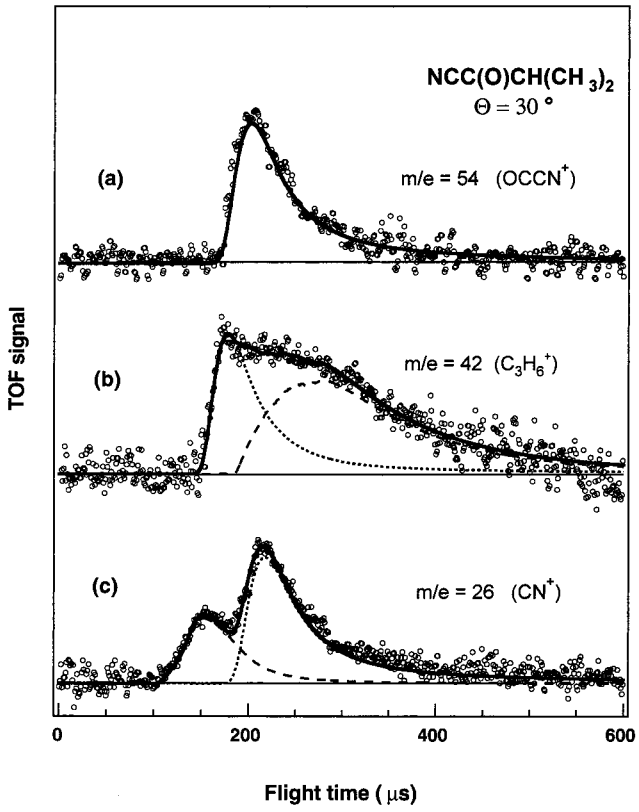

Figure 8. Unpolarized TOF spectra of the photofragments of isobutyryl cyanide after excitation at 193 nm for $OCCN^+$ (a), $C_3H_6^+$ (b), and CN^+ (c). The solid line in Figure 8a and the dotted lines in Figure 8b,c were calculated with the $P(E_T)$ from Figure 4c and the dashed lines in (b) and (c) with those from Figure 6c. The solid lines in (b) and (c) display the sum of the contributions from both decay channels.

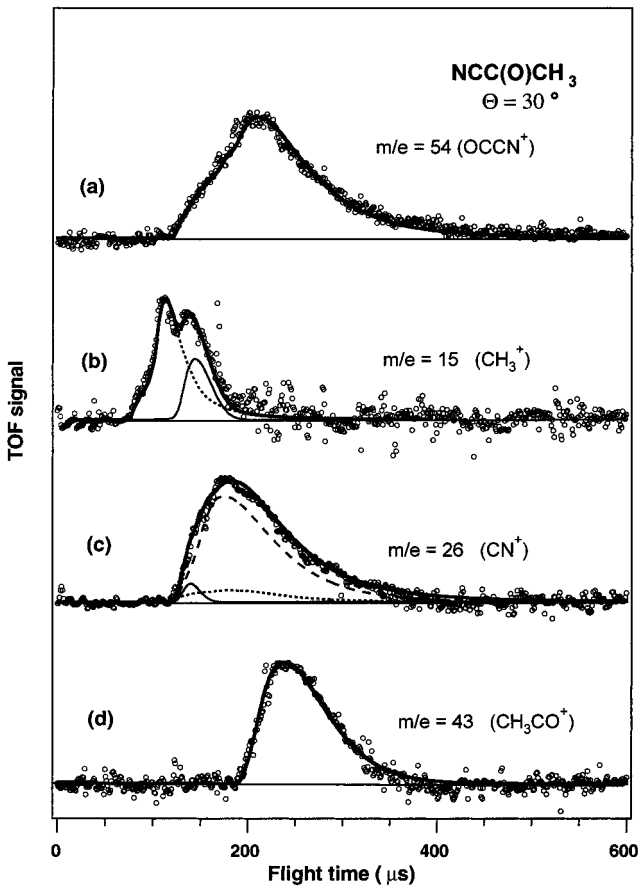

Figure 9. Unpolarized TOF spectra of the photofragments of acetyl cyanide after excitation at 193 nm for $OCCN^+$ (a), CH_3^+ (b), CN^+ (c), and CH_3CO^+ (d). The solid line in (a) and the dotted lines in (b) and (c) were calculated with the $P(E_T)$ from Figure 4d. The dashed line in (c) and the solid line in (d) were obtained with the $P(E_T)$ from Figure 6d. The solid lines in (b) and (c) display the sum of the contributions from both decay channels. The thin solid lines in (b) and (c) represent the contribution from the secondary dissociation of internally hot acetyl fragments.

especially for the slower fragments, we assume that the amount of OCCN having enough internal energy to decay spontaneously to CN and CO is less than 5%. The uncertainty for the H_9C_4-CO is probably larger as the slower CN radicals, corresponding to internally hot H_9C_4CO, may overlap with CN from fragmented OCCN in the TOF spectrum Figure 7c (region 185−275 μs) and therefore difficult to discern.

For isobutyryl cyanide (X = $CH(CH_3)_2$) we expect a similar photochemistry. Time-of-flight data of the photofragments were found at m/e = 54 ($OCCN^+$), 26 (CN^+), 42 ($C_3H_6^+$), and 70 ($H_6C_3CO^+$). Figure 8 shows the TOF spectra of the OCCN, CN, and C_3H_6 fragments. The data analysis was essentially the same as for pivaloyl cyanide (X = $C(CH_3)_3$). The $P(E_T)$ distribution of decay channel (2) leading to C_3H_7 and OCCN is displayed in Figure 4c. The corresponding fit to the spectra Figure 8b,c is represented by dotted lines and as a solid line in Figure 8a.

The agreement between the TOF spectra of OCCN and its alkyl counterfragment after momentum-matching was not satisfactory, implying that decay channel (1) and/or secondary dissociation of OCCN has to be taken into account. In contrast to the spectra of the methyl cyanoformate and pivaloyl cyanide where the small contribution of decay channel (1) overlapped with that from channel (2), the contribution of channel (1) is now evident in the TOF spectrum of the alkyl rest C_3H_6. The H_7C_3CO product was found to be partly cracked to H_6C_3 in the ionizer. We recorded the spectrum of the H_7C_3CO fragments as shown in Figure 5c and analyzed these data in combination with those of CN^+ from channel (1) in Figure 8c (first peak), according to the procedure described above. Figure 6c displays the resulting $P(E_T)$ distribution for channel (1), and its fit to the TOF spectra 8b,c is represented by dashed lines. Finally, the sum of the channel (1) and (2) contributions provided the overall fit (solid line) as displayed in the spectra of Figure 8. Using the same assumptions as for pivaloyl cyanide above, we estimated that about 70% of the excited parent molecules decay along channel (2) to OCCN + C_3H_7 and the remaining 30% along channel (1) to CN + H_7C_3CO. The excellent fit of all the TOF spectra based on only these two decays supports our expectation that the nascent OCCN and H_7C_3CO fragments are stable and do not undergo spontaneous decay.

Due to a 2−3 times smaller absorption cross section of pivaloyl and isobutyryl cyanide relative to methyl cyanoformate at 193 nm, the signal at the mass filter setting m/e = 28 (CO^+) was insufficient for an accurate measurement and also polarized measurements were qualitatively not satisfactory enough to determine recoil anisotropies.

D. TOF Spectra of $NCC(O)CH_3$. Acetyl cyanide (X = CH_3) is the only one of the four species which has been studied before.[15,16,21,22] Recently it has been investigated by North et al.[15] using high-resolution transient frequency modulation spectroscopy and photofragment translational energy spectroscopy. While in these experiments only the m/e = 26 (CN^+) could be recorded at a sufficient signal-to-noise ratio, we here report PTS spectra at m/e = 54 ($OCCN^+$), m/e = 26 (CN^+), m/e = 15 (CH_3^+), and m/e = 43 (H_3CCO^+). Cluster contribu-

tions to the signal could be neglected, as supported by the same TOF profiles obtained with and without a heated exit tubing (70 °C) attached to the piezoelectric valve. Figure 9 shows the TOF spectra of the detected fragments.

The unambiguous TOF spectrum of $OCCN^+$ was analyzed first. The center-of-mass kinetic energy distribution $P(E_T)$ obtained for the fragment pair from dissociation channel (2) is displayed in Figure 4d. The TOF spectrum of the counterfragment H_3C^+ given in Figure 9b shows clearly two separate components, a faster contribution with a maximum around 110 μs and a slower one around 135 μs. The first component (dotted line in Figure 9b) arises from primary methyl fragments since it is strictly momentum-correlated with stable OCCN represented by spectrum Figure 9a. Decay channel (1) is manifested by the one-component TOF spectrum of H_3CCO^+ (Figure 9d). The center-of-mass kinetic energy distribution $P(E_T)$ obtained from these H_3CCO data and shown in Figure 6d as a solid line was then applied to find the TOF spectrum of the counterfragment CN represented by the dashed line in Figure 9c. The agreement between the H_3CCO and CN data is apparently quite good, although two additional sources contribute to the CN^+ spectrum, namely fragmentation of $OCCN^+$ in the ionizer and CN as counterfragment of unstable acetyl. Before considering this we note that the $P(E_T)$ obtained by fitting the CH_3CO^+ spectrum peaks at very low kinetic energy which is compatible only with the formation of CH_3CO or CN in one of the energetically accessible excited electronic states. To extend the analysis accordingly, we must therefore distinguish between the formation of $CN + CH_3CO$ with both fragments being in the ground states (1a), or with CN in the excited A $^2\Pi$ state (110 kJ/mol,[37] 1b), or with CH_3CO in the excited A $^2A''$ state (145 kJ/mol,[38] 1c).

$$NCC(O)CH_3 + h\nu \rightarrow CN\ (X) + OCCH_3\ (X) \qquad \Delta H^0 = 457\ \text{kJ/mol} \quad (1a)$$

$$NCC(O)CH_3 + h\nu \rightarrow CN\ (A) + OCCH_3\ (X) \qquad \Delta H^0 = 567\ \text{kJ/mol} \quad (1b)$$

$$NCC(O)CH_3 + h\nu \rightarrow CN\ (X) + OCCH_3\ (A) \qquad \Delta H^0 = 602\ \text{kJ/mol} \quad (1c)$$

Since the CN spectrum (Figure 9c) exhibits no structure that would allow a clear distinction of two different CN contributions, we first analyzed the indirectly related H_3C spectrum Figure 9b which shows a bimodal TOF profile. The fast signal contribution (dotted line) was assigned above to H_3C as counterfragment to stable OCCN. The slower contribution at around 135 μs may arise from channel (2) (counterfragment to unstable OCCN), from fragmentation of acetyl in the detector, or from the spontaneous decay of acetyl radicals to $H_3C + CO$. Acetyl fragmentation in the detector can easily be dismissed since the flight time of the observed signal contributions given as a thin solid line is too short. The possibility of slower H_3C^+ radicals as counterfragment to unstable and not-detected OCCN was also dismissed on the basis of the internal energy estimate of the OCCN fragment (see discussion) which reveals OCCN to be essentially stable. We conclude therefore that the slower H_3C^+ component (thin solid line in Figure 9b) is due to formation of $CN + CH_3CO$ in their ground states (1a), followed by a secondary decay of acetyl radicals to $H_3C + CO$. The primary $P(E_T)$ of the ground-state channel (1a) is expected to be different from that of channel (1b) and (1c) where the latter was found by fitting the stable CH_3CO^+ signal. The former cannot be determined unambiguously from our data set since the CN^+ spectrum is unstructured and the primary CH_3CO formed in reaction 1a is believed to decay before reaching the detector. However, it is reasonable to assume that the average kinetic energy $\langle E_T \rangle$ of the fragment pair from channel (1a) is larger than in (1b) and (1c) owing to the substantially higher available energy. Therefore the upper end of the primary $P(E_T)$ of channel (1a) was adjusted to fit the rising edge of the CN^+ spectrum, while the width of the distribution was varied iteratively together with the secondary $P(E_T)$ of the unstable CH_3CO until a good agreement with the slow CH_3^+ signal component was achieved (thin solid lines in Figure 9b,c). The final primary $P(E_T)$ for reaction 1a is shown as a dashed line in Figure 6d, and the CN counterfragment contribution is represented as a thin solid line in Figure 9c. The spontaneous secondary decay of acetyl was treated with the procedure described in refs 39−41 using a kinetic energy distribution of the $H_3C + CO$ pairs symmetrically centered at 60 kJ/mol (fwhm = 20 kJ/mol) and a forward−backward symmetric angular distribution. The difficulty in determining the primary $P(E_T)$ of (1a) does not justify a refined fit of the secondary decay process.

The CN^+ spectrum in Figure 9c was used to inspect the results from the other three species (OCCN, H_3CCO, and H_3C). The CN signal might contain contributions of primary CN from decay channel (1) correlating to stable and unstable acetyl, CN from OCCN cracked in the detector, and CN from spontaneous decay of internally hot OCCN. Since the OCCN fragments can be regarded as an essentially stable species with respect to secondary decay, we are left with three contributions constituting the CN spectrum of Figure 9c. The cracking contribution from OCCN (dotted line) was found by appropriate scaling of the $OCCN^+$ signal corrected for the OCCN cracking ratio. The ratio of the contributions from CN coincident with stable CH_3CO (dashed line) and CN coincident with unstable CH_3CO (thin solid line), which together constitute the rest of the CN^+ signal, was evaluated by comparison of the signal strengths at m/e = 43 (CH_3CO^+) and the slow contribution in the m/e = 15 (CH_3^+) spectrum. Considering the ratio of the ionization efficiencies $CH_3CO/CH_3 \sim 1.6$ we find that about 9% of the acetyl fragments are unstable, while 91% are stable and must be formed by channel (1b) or (1c) (see Discussion). The overall fits of the spectra in Figure 9b,c, indicated by a solid line, represent the sum of all these contributions.

A rough estimate of the branching ratio channel (1)/channel (2) was obtained by comparison of the relative signal intensities of the two primary dissociation products CH_3CO (representing channel (1)) and OCCN (representing channel (2)). If all secondary decay processes are neglected and a ratio of ionization efficiencies for CH_3CO to OCCN of ~1.1 is used as calculated from the sum of the atomic polarizabilities,[42] we find a ratio channel (1)/channel (2) ~ 5. This ratio was inspected by comparing the signal strengths of OCCN (m/e = 54) and primary CN (dashed + thin solid lines in m/e = 26 spectrum). After consideration of the known OCCN cracking pattern and the relative ionization efficiencies, a branching ratio channel (1)/channel (2) ~ 5.7 was calculated, in good agreement with the value obtained above.

In summary, about 15% of the excited acetyl cyanide molecules decay along channel (2) to $OCCN + CH_3$, and about 85% along channel (1) to $CH_3CO + CN$. Roughly 9% of the nascent acetyl radicals from channel (1) are unstable and subject to secondary dissociation to $CH_3 + CO$.

TABLE 2: Fragment Energy Partitioning for Decay Channel NCC(O)X → OCCN + X (2) of the Photodissociation of NCC(O)X at 193 nm and Dissociation Energies

E [kJ/mol]	X = CN	X = CH_3	X = $CH(CH_3)_2$	X = $C(CH_3)_3$	X = OCH_3
$E_{T,max}$	139 ± 8	265 ± 10	97 ± 5	77 ± 5	105 ±2
$h\nu - E_{T,max}$	480 ± 8	354± 10	522 ± 5	542 ± 5	514 ± 2
D_0(NCC(O)−X)[a]	410	377	375	336	436
$\langle E_T \rangle$	40 ± 5	80 ± 6	50 ± 4	32 ± 2	67 ± 1
$\langle E_{int} \rangle / E_{avl}$					
experiment	0.81	0.67	0.80	0.89	0.63
prior distribution	0.86	0.91	0.96	0.97	0.92

[a] CBS-4, ± 15 kJ/mol.[44]

4. Discussion

Our study shows that the photodissociation of the investigated NCC(O)X molecules at 193 nm proceeds via two decay paths, (1) to XCO + CN and (2) to OCCN + X. The branching ratio between the two decay channels varies depending on the nature of the X substituent. No evidence was found for a molecular channel (3). Furthermore, from the poor agreement between our experimental PTS data and fits assuming a simultaneous scission of both C−C bonds, we conclude a synchronous three-body decay to be unimportant.

Channel (2): NCC(O)X → NCCO + X. The $P(E_T)$ distributions of channel (2) shown in Figure 4 can be characterized by the maximum kinetic energy $E_{T,max}$ (indicated by arrows) and the average kinetic energy $\langle E_T \rangle$ of the fragment pairs X + OCCN. The $E_{T,max}$ and $\langle E_T \rangle$ values of the investigated NCC(O)X compounds are summarized in Table 2. Previously obtained values for the related carbonyl cyanide[20] are also given for comparison. We start with a consideration of the bond energies of the investigated molecules followed by a discussion of the average kinetic energies and—if available—the recoil anisotropies with respect to a possible dissociation mechanism.

The high-energy threshold of the translational energy distribution provides an upper limit for the dissociation energy D_0:

$$D_0 \leq h\nu - E_{T,max} \tag{5}$$

where the equality sign applies when the coldest fragments are formed in the rovibrational ground state. From the fastest TOF fragments it is therefore often feasible to determine D_0. In Table 2, the thus determined D_0 values are given together with results from recent CBS-4 ab initio calculations.[43,44] Horwitz et al.[16] also calculated dissociation energies for CH_3 and CN elimination from acetyl cyanide and obtained values of 359 and 427 kJ/mol, respectively, roughly 5% lower than Suter's values.[44] The comparison supports the estimated absolute accuracy of the calculated values to ±20 kJ/mol. However, the error between *differences* in the bond energies using one particular ab initio basis set is expected to be smaller than about 5 kJ/mol for the related molecules presented in this study.

According to the CBS-4 calculations the energy required to break the C−X bond is smallest for X = *tert*-butyl consistent with the common rule used in chemistry that *tert*-butyl is a "good leaving group". The larger dissociation energies for X elimination from NCC(O)X, X = CN and X = CH_3O, compared to those for X elimination from NCC(O)X, X = alkyl, reflect the partial conjugation with the π system of the carbonyl moiety (Table 2). With the exception of acetyl cyanide to CH_3 + OCCN, where the experimental value of D_0 = 354 kJ/mol and calculated values of D_0 = 359 kJ/mol[16] and 377 kJ/mol[44] are close, the deviations between the values for D_0 from eq 5 and those from the ab initio calculations are substantial. While in the former decay the fastest fragments are indicated to be internally cold, this is not the case for the other decays. For isobutyryl and pivaloyl cyanide even the fastest fragment pairs OCCN + X, X = isopropyl and *tert*-butyl possess internal excitation of 147 and 206 kJ/mol, respectively. The fraction of E_{avl} partitioned into internal energy of X apparently increases with the number of vibrational degrees of freedom of X (6, 24, and 33 for X = methyl, isopropyl, and *tert*-butyl, respectively).

The average internal energies were obtained with the relationship

$$\langle E_{int} \rangle = h\nu - D_0 - \langle E_T \rangle \tag{6}$$

using the ab initio dissociation energies[44] in Table 2. The fractions of the internal excitation of the fragments to the available energy, $\langle E_{int} \rangle / E_{avl}$, are given in Table 2. These values are compared to the internal energy release obtained with the prior model,[45] which assumes equipartitioning of E_{avl} over all internal degrees of freedom for barrierless dissociation on the ground-state potential energy surface. All compounds show the experimentally determined average internal excitation to be smaller than predicted by this statistical model. The smallest difference between experimental and prior values is found for X = $C(CH_3)_3$ and taken as evidence for the statistical character of the decay process. The largest discrepancy appears for the X = OCH_3 compound, where only 63% of E_{avl} is channeled into internal excitation, compared to 92% for a purely statistical decay. However, the results for methyl cyanoformate are not directly comparable with those of the cyano acyl compounds as the methoxy species is an ester, whereas the alkyl species investigated are ketones. Additional evidence for a nonstatistical decay of the ester compound is the anisotropic recoil distribution of the fragments OCCN + OCH_3 with $\beta = 0.8 \pm 0.1$ which implies a fast separation of the fragments (<1 ps[36]) on the time scale of parent rotation (for details see ref 46). Within the homologous series X = methyl, isopropyl, and *tert*-butyl the trend toward increasing internal energy with increasing size of the alkyl fragment is in qualitative agreement with the expectation for a statistical decay. (It is noted that even for fully statistical processes the simple prior model gives only an upper limit to E_{int} since it overestimates the vibrational excitation of the high-frequency vibrational modes.[45])

The spontaneous secondary dissociation of OCCN to CN + CO fragments was found to be unimportant (≤5%) for all the present NCC(O)X compounds. In our previous study on $CO(CN)_2$ about 18% of the primary OCCN radicals were shown to undergo such a decay.[20] The smaller internal energy and hence the higher stability of OCCN formed from NCC(O)X, X = methyl, isopropyl, *tert*-butyl, is attributed to the larger "heat bath" provided by the X moiety in accordance to a statistical decay. From the prior model the upper limit to the internal excitation of OCCN formed from carbonyl cyanide is estimated to be E_{int}^{prior}(OCCN) = 142 kJ/mol thus lying above the dissociation energy D_0(OC−CN) = 126 kJ/mol,[16] while for all the other compounds E_{int}^{prior}(OCCN) < D_0(OC−CN). This confirms our experimental results of stable OCCN fragments produced by elimination of X = methyl, isopropyl, *tert*-butyl and of the decay of a fraction of the OCCN fragments from $CO(CN)_2$. The OCCN fragments emerging from methyl cyanoformate are additionally stabilized by the comparatively large amount of excess energy channeled into fragment recoil E_T.

Channel (1): NCC(O)X → NC + XCO. The $P(E_T)$ distributions of the CN elimination channel (1) are displayed in Figure 6 and their characteristic $\langle E_T \rangle$ and $E_{T,max}$ values are

TABLE 3: Fragment Energy Partitioning for Decay Channel NCC(O)X → XCO + CN (1) of the Photodissociation of NCC(O)X at 193 nm and Dissociation Energies

E [kJ/mol]	X = CN	X= CH_3	X = $CH(CH_3)_2$	X = $C(CH_3)_3$	X = OCH_3
$E_{T,max}$	139 ± 8	43 ± 5	170 ± 14	211 ± 10	215 ± 23
$h\nu - E_{T,max}$	480 ± 8	576 ± 5	449 ± 14	408 ± 10	404 ± 23
D_0(NC−C(O)X)[a]	410	457	463	423	483
$\langle E_T \rangle$	40 ± 5	10 ± 2 22 ± 2[b]	56 ± 2	79 ± 2	67 ± 2
$\langle E_{int} \rangle / E_{avl}$					
experiment	0.81	0.94 0.86[b]	0.64	0.60	0.51
prior distribution	0.86	0.91	0.96	0.97	0.92
D_0(X−CO)[a]	131	50	43	44	

[a] CBS-4, ± 15 kJ/mol.[44] [b] Ground-state channel (1a).

listed in Table 3 together with calculated dissociation energies for primary and secondary decays.

According to the ab initio calculations,[44] CN elimination requires more energy than elimination of the X group, the difference between the C−X and C−CN bond dissociation energies being ∼85 kJ/mol for X = methyl, isopropyl, *tert*-butyl, and ∼47 kJ/mol for X = methoxy (cf. Tables 2 and 3). The fraction of available energy deposited into internal excitation of CN + OCX is relatively low for isobutyryl cyanide (64%), pivaloyl cyanide (60%), and methyl cyanoformate (51%) as compared to translational motion which indicates that in these dissociation processes the excess energy is not randomized. However, a surprising result is the high internal energy of 152 kJ/mol for CN fragments formed in coincidence with *stable* acetyl radicals which corresponds to 94% of the available energy. (This even exceeds the predicted 91% for a prior distribution.) Previous measurements have shown that acetyl decomposes to CH_3 + CO when the internal energy exceeds the barrier of 71 kJ/ mol.[8,47] Since $\langle E_{int} \rangle$ ∼152 kJ/mol is far above this barrier and the CN fragments should acquire only a minor fraction of the total internal energy, we have to consider the formation of one of the fragments in an electronically excited state in order to explain the stability of the acetyl fragments. As mentioned in section 3, energetically feasible excitations are (1b), with CN in the A $^2\Pi$ state (110 kJ/mol[37]), or (1c), with acetyl in the A $^2A''$ state (145 kJ/mol above the X $^2A'$ ground state[38]).

The $P(E_T)$ curve determined for CN in combination with unstable CH_3CO (dashed line in Figure 6) exhibits an average recoil energy of about 22 kJ/mol, somewhat lower than the value $\langle E_T \rangle$ = 30.5 kJ/mol measured by North et al.[15] who used transient frequency modulation spectroscopy to probe the nascent CN radicals in the electronic ground state. The discrepancy may be due to our difficulty, and in turn to the uncertainty, in determining the individual distributions for the primary and secondary decays of unstable acetyl from the TOF data. According to our estimates approximately 9% of the acetyl fragments are unstable and undergo secondary dissociation to CH_3 + CO, while 91% remain stable. These fractions also reflect the branching between the ground-state channel (1a) and the excited-state channels (1b) and (1c), since in the ground-state channel the large E_{int} of 119−162 kJ/mol (based on D_0 = 457 kJ/mol[44]) should result in complete secondary decay of CH_3-CO while in the excited states no secondary decay is expected. (The available energies in the excited states (1b) and (1c) are calculated to be 52 and 17 kJ/mol, respectively, if the dissociation energy D_0 = 457 kJ/mol[44] is used, and 82 and 47 kJ/mol, respectively, for D_0 = 427 kJ/mol[16]).

TABLE 4: Branching of the Decay Channels (1) and (2) to the Photodissociation of NCC(O)X at 193 nm

X	OCCN + X	CN + OCX
CH_3	15 ± 10%	85 ± 10%
$CH(CH_3)_2$	70 ± 10%	30 ± 10%
$C(CH_3)_3$	83 ± 10%	17 ± 10%
OCH_3	95 ± 2%	5 ± 2%

In contrast to acetyl cyanide, the secondary decay of the acyl fragments C_3H_7CO and C_4H_9CO was found to be insignificant. The "higher" stability of these fragments compared to acetyl is attributed to a greater release of translational energy and a higher potential to accommodate the internal excitation on the many vibrational degrees of freedom. Although electronic excitation of the C_3H_7CO + CN and C_4H_9CO + CN fragment pairs is also possible, such channels would be at most of minor importance because only the slowest fragment pairs which constitute a minor fraction of the total $P(E_T)$ would be compatible with electronically excited fragment species.

The efficiency of the CN elimination channel (1) was found to decrease from about 85% for acetyl cyanide to 13% for the pivaloyl cyanide (Table 4). Thus increasing the size of the alkyl group not only stabilizes the nascent OCCN radical, but also shifts the branching ratio of the two competitive reactions in favor of channel (2). This shift might be explained by a larger decrease of the dissociation barrier height of channel (2) relative to channel (1) with increasing size of the alkyl group. It is clearly not due to changes in the dissociation energies as for all three compounds the C−X bond is weaker than the C−CN bond by the same, constant amount of ≈80 kJ/mol. From the dissociation energies we therefore should expect that channel (2) is the major decay channel in all compounds presented in this study, including methyl cyanoformate which exhibits the strongest propensity for this decay route, in this case the OCH_3 elimination.

5. Conclusions

In this study the photodissociation of four cyano carbonyl compounds NCC(O)X at 193 nm was investigated. Triggered by recent reports according to which the stronger C−C bond in acetyl cyanide (X = CH_3) is selectively broken,[15,16] we focused on changes in this selectivity as the group X is replaced by isopropyl, *tert*-butyl, and methoxy. Table 4 summarizes the results. Acetyl cyanide is the only compound in which the energetically less favorable CN elimination reaction (channel 1) dominates over the alkyl elimination. With increasing size of the alkyl group the propensity for CN elimination is lost and OCCN + alkyl are the major photoproducts. This change in propensity is not evident from the energetics, since *both* the C−CN and the C−X bond are weakened as the alkyl group increases in size. We speculate that the formation of electronically excited CN or acyl, which was only found to be a major channel for acetyl cyanide [channels (1b) and (1c)], may be related to the preferred CN bond breaking in this compound. The photodissociation of methyl cyanoformate showed a strong preference for elimination of the methoxy group although both bonds have comparable dissociation energies. This strong propensity is consistent with similar results of the chemically related acetic acid.

Spontaneous secondary decay has only be found for acetyl cyanide, where part of the primary CH_3CO fragments possess sufficient internal energy to pass the barrier to CH_3 + CO. Provided that the excess energy is at least partially randomized among all internal degrees of freedom, it is clear that with

increasing size of the X group the stability of nascent COX increases. In addition, those decay processes which release a large fraction of excess energy as fragment recoil, such as methyl cyanoformate, are also expected to form cold and stable fragments.

With respect to our initial goal of maximizing the yield of *stable* OCCN radicals, we were successful with two approaches. (i) The larger the alkyl group X, the more internal degrees of freedom are supplied, thus preventing a large fraction of E_{int} from being deposited on OCCN. (ii) The preferred deposition of available energy into translational motion of the fragments as in methyl cyanoformate provided an almost clean source of OCCN + OCH_3. The strong propensity here may also be attributed to a decay mechanism similar to that found for acetic acid, where the scission of the stronger C−O bond is enhanced by an adiabatic decay pathway, while dissociation of the C−C bond requires a slow intersystem crossing.

Acknowledgment. This work was supported by the Swiss National Science Foundation and the Alfred Werner Legat. The authors thank Rolf Pfister for the synthesis of isobutyryl cyanide and Dr. R. T. Carter for carefully reading the manuscript.

References and Notes

(1) Noyes, W. A. *Photochemistry and reaction kinetics*; Cambridge University Press: Cambridge, 1967.
(2) Turro, N. J. *Modern molecular photochemistry*; University Science Books: Mill Valley, 1991.
(3) Reinsch, M.; Klessinger, M. *J. Phys. Org. Chem.* **1990**, *3*, 81.
(4) Calvert, J. G.; Pitts, J. N. *Photochemistry*; Wiley: New York, 1966.
(5) Person, M. D.; Kash, P. W.; Butler, L. J. *J. Chem. Phys.* **1992**, *97*, 355.
(6) Person, M. D.; Kash, P. W.; Butler, L. J. *J. Phys. Chem.* **1992**, *96*, 2021.
(7) North, S.; Blank, D. A.; Lee, Y. T. *Chem. Phys. Lett.* **1994**, *224*, 38.
(8) Arunan, E. *J. Phys. Chem. A* **1997**, *101*, 4838.
(9) Lane, I. C.; Meehan, R.; Powis, I. *J. Phys. Chem.* **1995**, *99*, 12371.
(10) North, S. W. Thesis, University of California, 1995.
(11) Kroger, P. M.; Riley, S. J. *J. Chem. Phys.* **1977**, *67*, 4483.
(12) Hunnicutt, S. S.; Waits, L. D.; Guest, J. A. *J. Phys. Chem.* **1989**, *93*, 5188.
(13) Hunnicutt, S. S.; Waits, L. D.; Guest, J. A. *J. Phys. Chem.* **1991**, *95*, 562.
(14) Peterman, D. R.; Daniel, R. G.; Horwitz, R. J.; Guest, J. A. *Chem. Phys. Lett.* **1995**, *236*, 564.
(15) North, S. W.; Marr, A. J.; Furlan, A.; Hall, G. E. *J. Phys. Chem. A* **1997**, *101*, 9224.
(16) Horwitz, R. J.; Francisco, J. S.; Guest, J. A. *J. Phys. Chem.* **1997**, *101*, 1231.
(17) Smith, D.; Adams, N. G. *J. Chem. Soc., Faraday Trans. 2* **1989**, *85*, 1613.
(18) Seibert, J. W. G.; Winnewisser, M.; Winnewisser, B. P. *J. Mol. Spectrosc.* **1996**, *180*, 26.
(19) Furlan, A.; Scheld, H. A.; Huber, J. R. *Chem. Phys. Lett.* **1998**, *282*, 1.
(20) Scheld, H. A.; Furlan, A.; Huber, J. R. *J. Chem. Phys.* **1999**, *111*, 923.
(21) Sumathi, R.; Nguyen, M. T. *J. Phys. Chem. A* **1998**, *102*, 412.
(22) So, S. P. *Chem. Phys. Lett.* **1997**, *270*, 363.
(23) Maul, C.; Gericke, K.-H. *Int. Rev. Phys. Chem.* **1997**, *16*, 1.
(24) Strauss, C. E. M.; Houston, P. L. *J. Phys. Chem.* **1990**, *94*, 8751.
(25) Felder, P. *Chem. Phys.* **1990**, *143*, 141.
(26) Hoffmann, H. M. R.; Haase, K. *Synthesis* **1981**, 715.
(27) Haase, K.; Hoffmann, H. M. R. *Angew. Chem.* **1982**, *94*, 80.
(28) Robin, M. B. *Higher Excited States of Polyatomic Molecules*; Academic: New York, 1975; Vol. 2.
(29) Gaines, G. A.; Donaldson, D. J.; Strickler, S. J.; Vaida, V. *J. Phys. Chem.* **1988**, *92*, 2762.
(30) Baba, M.; Hanazaki, I.; Nagashima, U. *J. Chem. Phys.* **1985**, *82*, 3938.
(31) Owrutsky, J. C.; Baronavski, A. P. *J. Chem. Phys.* **1999**, *111*, 7329.
(32) Sparks, R. K.; Shobatake, K.; Carlson, L. R.; Lee, Y. T. *Chem. Phys.* **1981**, *75*, 3838.
(33) Wodtke, A. M.; Hintsa, E. J.; Lee, Y. T. *J. Chem. Phys.* **1986**, *84*, 1044.
(34) Yarkony, D. R. *J. Am. Chem. Soc.* **1992**, *114*, 5406.
(35) Keller, B. A.; Felder, P.; Huber, J. R. *J. Phys. Chem.* **1987**, *91*, 1114.
(36) Jonah, C. *J. Chem. Phys.* **1971**, *55*, 1915.
(37) Huber, K. P.; Herzberg, G. *Molecular Spectra and Molecular Structure IV. Constants of Diatomic Molecules*; Van Nostrand: New York, 1979.
(38) Mao, W.; Li, Q.; Kong, F.; Huang, M. *Chem. Phys. Lett.* **1998**, *283*, 114.
(39) Zhao, X.; Nathanson, G. M.; Lee, Y. T. *Acta Physico-Chim. Sinica* **1992**, *8*, 70.
(40) Hintsa, E. J.; Zhao, X.; Lee, Y. T. *J. Chem. Phys.* **1990**, *92*, 2280.
(41) Felder, P. Habilitation, University of Zürich, 1993.
(42) Krajnovich, D.; Butler, L. J.; Lee, Y. T. *J. Chem. Phys.* **1984**, *81*, 3031.
(43) Ochterski, J. W.; Petersson, G. A.; Montgomery, J. A. *J. Chem. Phys.* **1996**, *104*, 2598.
(44) Suter, H.-U. To be published.
(45) Zamir, E.; Levine, R. D. *Chem. Phys.* **1980**, *52*, 253.
(46) The sign of the β value of the fragments OCCN + OCH_3 provides some information about the nature of the electronic excitation of methyl cyanoformate at 193 nm. Assuming that between the CO, the CN and the OCH_3 groups in $NCC(O)OCH_3$ all bond angles are 120°, (cf. Figure 1) an orientation of the transition dipole moment μ in the plane of OCCN yields a limiting β value of −0.25 if μ lies parallel to the C═O bond, and +1.25 if μ is perpendicular to C═O. For μ perpendicular to the OCCN plane the limiting value is $\beta = -1$. The measured anisotropy is most compatible with μ in the plane and perpendicular to C═O, similar to $CO(CN)_2$ where the corresponding excited state is of B_2 symmetry.
(47) Watkins, K. W.; Word, W. *Int. J. Chem. Kinet.* **1974**, *6*, 855.